7 The bow shock and the magnetopause

We have seen in our discussion of the solar wind that it is supersonic; typically with Mach numbers of the order of 10. In this section we will discuss how the supersonic flow interacts with an obstacle such as the Earth's magnetic field.

7.1 Shock waves

In any medium information is propagating with a characteristic velocity; sound, for example, is information in the form of a compressional wave traveling with the speed of sound.

In the left part of Fig. 1 shows the scenario where the information speed c_s is larger than the object speed u; after three time steps Δt the information (sound wave) is still ahead of the object, giving the medium time to move out of the way.

If an object is traveling at a speed faster than the local speed of the information "an object is coming", e.g., the local sound speed, the medium in front of the object would not be able to receive this information in order to move out of the way before the object has reached it. This scenario is shown on the right in Fig. 1; after three time steps Δt the object is ahead of the information. But clearly, we have supersonic airplanes that can travel faster than the speed of sound, so how does the air "know" to move out of the way?

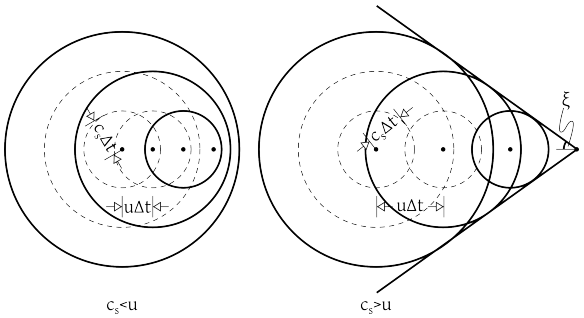

Figure 1: On the left the subsonic scenario, on the right the supersonic scenario.

Of course, the above sscenario is equivalent to a stationary object and the medium flowing over it; this is typically the coordinate system which is used in the terrestrial system, i.e., the Earth is stationary and the solar wind blows across it. If the flow is supersonic, a shock wave is set up in front of the object. This shock wave involves irreversible processes (sound waves are adiabatic) and it changes medium's characteristica (temperature, density, flow speed), such that the flow is subsonic behind it (see Fig. 2).

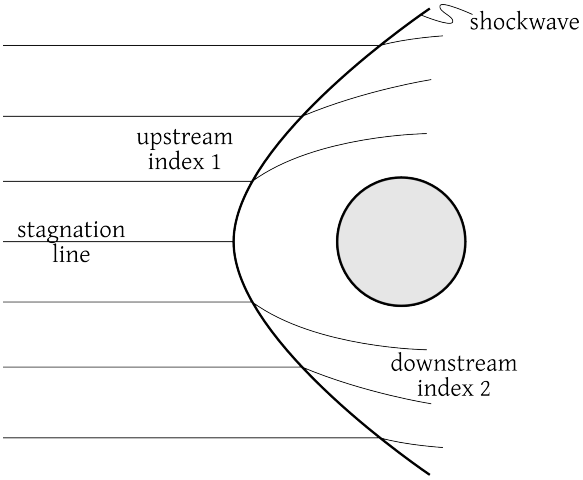

Figure 2: Supersonic flow in the upstream region is slowed to subsonic speeds in the downstream region by a shock wave.

The change in state can be calculated from conservation laws, as mass, momentum, and energy are conserved across the shock. Consider the situation in Fig. 3 for which the three conserved quantities can be expressed as:

$$\rho_1 v_1 = \rho_2 v_2 \tag{7.1}$$

$$\rho_1 v_1^2 + p_1 = \rho_2 v_2^2 + p_2 \tag{7.2}$$

$$\rho_1 e_1 v_1 + p_1 v_1 = \rho_2 e_2 v_2^2 + p_2 v_2. \tag{7.3}$$

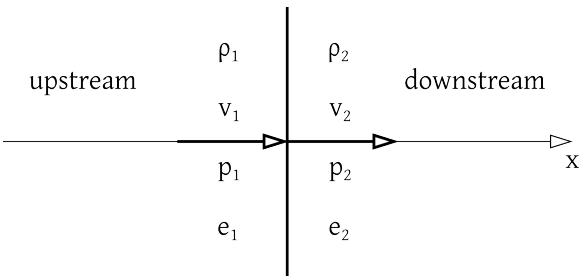

Figure 3: Schematic to derive the jump conditions.

After a lengthy calculation and observing that the internal energy of an ideal gas ($p = \rho RT = \rho(\gamma-1)c_vT$) is the sum of thermal and kinetic energy, i.e., $e = c_vT + v^2/2$, we arrive at the change in pressure as a function of the polytropic index γ and the upstream Mach number M_1:

$$\frac{p_2}{p_1} = \frac{2\gamma M_1^2 - (\gamma-1)}{\gamma+1}. \tag{7.4}$$

The actual obstacle around which the solar wind has to flow, however, is not the Earth itself but its magnetic field (frozen-in theorem). To derive the pressure the solar wind exerts on the dayside magnetic field, consider the stagnation streamline, which is the streamline at which the flow speed drops to zero:

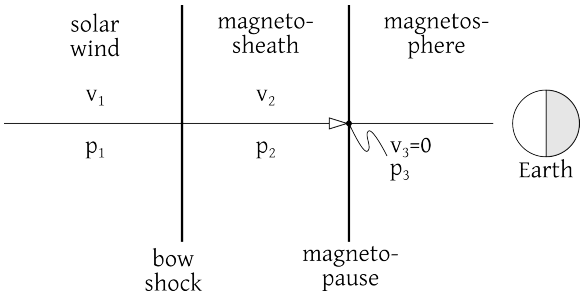

Figure 4: Stagnation streamline.

Along this streamline in the magnetosheath, the flow is subsonic and Bernoulli's relation holds along the entire streamline such that:

$$\frac{v^2}{2} + \frac{\gamma}{\gamma-1}\frac{p}{\rho} = \text{const.} \tag{7.5}$$

or, because we are considering the stagnation streamline where $v_3 = 0$

$$\frac{v_2^2}{2} + \frac{\gamma}{\gamma-1}\frac{p_2}{\rho_2} = \frac{\gamma}{\gamma-1}\frac{p_3}{\rho_3}. \tag{7.6}$$

From eq. (7.6) we can derive the ratio of p_2 and p_3, i.e., the pressure the medium in the magnetosheath exerts on the terrestrial magnetic field at the stagnation point. having derived a relation between p_2 and p_3, we can express p_2 in terms of p_1 using eq. (7.4):

$$p_3 = K\rho_1 v_1^2 \tag{7.7}$$

with

$$K = \frac{1}{\gamma M_1^2}\frac{2\gamma M_1^2 - (\gamma-1)}{\gamma+1} \left[1 + \frac{\gamma-1}{2}\frac{2+(\gamma-1)M_1^2}{2\gamma M_1^2 - (\gamma-1)}\right]^{\gamma/\gamma-1}. \tag{7.8}$$

For typical values of the solar wind, $K \approx 0.88$, showing that the dynamic pressure of the solar wind is converted to thermal pressure along the stagnation streamline.

7.2 Earth's magnetic field

In 1839 Carl-Freidrich Gauß realized that the magnetic field $\vec{B}$ in a source-free region, i.e., where $\vec{j} = 0$, is described by a simplified Ampère's law

$$\nabla \times \vec{B} = 0 \tag{7.9}$$

such that $\vec{B}$ can be expressed as the gradient of a scalar potential $\vec{B} = -\nabla V$. This potential could be separated into an external part V_{ext}, due to currents flowing above the source-free region, and and internal part V_{int} due to currents flowing below it.

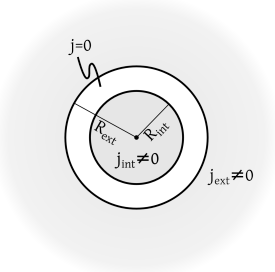

Figure 5: Schematic showing how the magnetic field in the source-free region can be derived from the superposition of the internal and external potentials.

Of course $\nabla \cdot \vec{B} = 0$ holds such that the potential must fullfil Laplace's equation $\nabla^2 V = 0$. In spherical corrdinates the solution to Laplace's equation are the well-known spher-

ical harmonics. Therefore

$$\begin{aligned} V &= V_{int} + V_{ext} \\ &= R_{int} \sum_{n=1}^{N_{int}} \left(\frac{R_{int}}{r}\right)^{n+1} \\ &\quad \sum_{m=0}^{n} \left(g_n^m \cos m\lambda + h_n^m \sin m\lambda\right) P_n^m(\cos\varphi) \\ &\quad + R_{ext} \sum_{n=1}^{N_{ext}} \left(\frac{r}{R_{ext}}\right)^{n} \\ &\quad \sum_{m=0}^{n} \left(q_n^m \cos m\lambda + s_n^m \sin m\lambda\right) P_n^m(\cos\varphi) \end{aligned} \tag{7.10}$$

where $P_n^m(x)$ are the associated Schmid-normalized Legendre polynomials. g_n^m, h_n^m, q_n^m, and s_n^m are the constants of the sperical harmonic expansion of the internal and external potentials from which the Earth's magnetic field can be derived in the source-free region. Using magnetic field measurements from many places in the world, Gauß was able to show that

$$g_n^m, h_n^m \gg q_n^m, s_n^m \tag{7.11}$$

indicating that the surface magnetic field has its sources mainly below the planet's surface. Once we have the spherical harmonic expansion of the scalar potential, we can derive the magnetic field components - to first order:

$$B_r(r,\lambda,\varphi) = -\frac{\partial V_{int}}{\partial r} = 2g_1^0 \left(\frac{R_e}{r}\right)^3 \cos\varphi \tag{7.12}$$

$$B_\lambda(r,\lambda,\varphi) = 0 \tag{7.13}$$

$$B_\varphi(r,\lambda,\varphi) = -\frac{1}{r}\frac{\partial V_{int}}{\partial \varphi} = g_1^0 \left(\frac{R_e}{r}\right)^3 \sin\varphi \tag{7.14}$$

This describes, of course, a dipole magnetic field with

$$\begin{aligned} |B| &= \sqrt{B_r^2 + B_\varphi^2} \\ &= g_1^0 \sqrt{1+3\cos^2\varphi} \left(\frac{R_e}{r}\right)^3 \end{aligned} \tag{7.15}$$

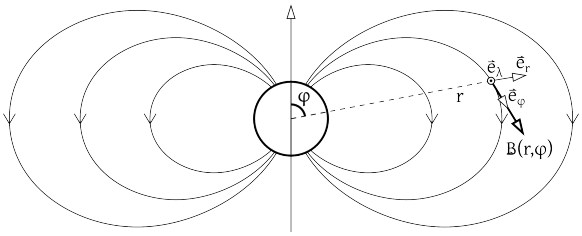

Figure 6: Magnetic dipole and spherical coordinates.

From the International Geomagnetic Reference Field (IGRF) we know that in 2010 $g_1^0 = -29496.5$ nT such that the direction of the magnetic field of Earth is actually reversed to that shown in Fig. 6. The jovian magnetic field, however, is aligned as shown in Fig. 6.

7.3 The magnetopause

At the interface between the magnetospheath and the terrestrial magnetic field - this boundary is called the magnetopause - we find that the magnetic field strength in the magnetosheath B_{MS} is only about 1% of the field strength measured inside of the magnetopause B_{MP}. This requires a current to flow in the boundary layer. This current is called the Chapman-Ferraro current and its strength is such that inside the magnetopause the magnetic field strength is about twice that of the expected dipole strength, $B_{MP} \approx 2B_{dip}$.

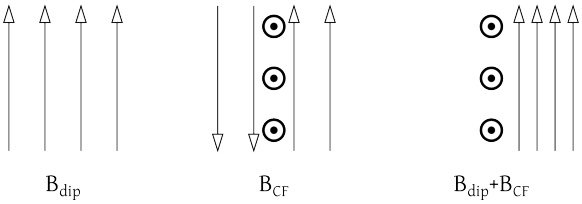

Figure 7: Chapman-Ferraro current on the magnetopause, looking from the side.

There is also a physical reason for the Chapman-Ferraro current. Consider positively charged ions comprising the solar wind as they cross from a region of relatively low

magnetic field strength (the magnetosheath) into a region of strong magnetic fields (the dayside magnetosphere). In the low magnetic field strength region the gyroradius will be very larger such that there the particle will almost move in a straight line. Once it enters the high magnetic field strength region, however, its gyroradius will become much smaller; after half a gyration it will then exit the high magnetic field strength region and again travel in a straight line. The same is of course true for electrons.
However, because the direction of gyration is opposite for ions and electrons, the two will, during their brief excursion into the high magnetic field strength region move in opposite directions, thus creating a net current.

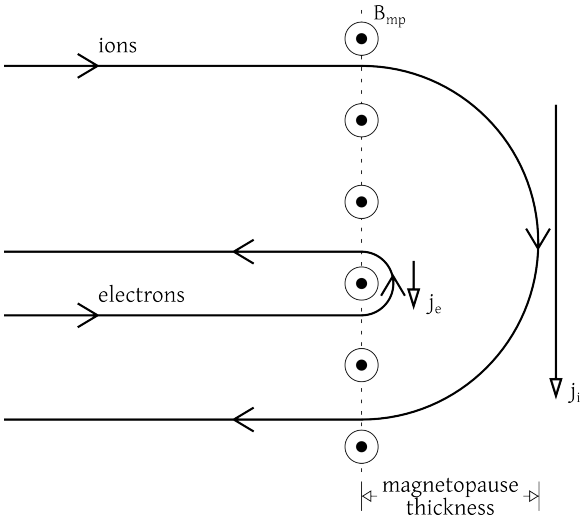

Figure 8: Physical explanation of the Chapman-Ferraro current on the magnetopause, looking down onto the magnetopause.

Across the entire magnetopause the pressure exerted by the solar wind is balanced by the magnetic pressure of the dipole field. In the equatorial plne, where the stagnation streamline is located, we can use eq. (7.7) to estimate the steady state pressure balance:

$$K\rho_{SW}v_{SW}^2 = \frac{B_{MP}^2}{2\mu_0} = \frac{2B_{dip}^2}{2\mu_0}. \qquad (7.16)$$

The magnetic dipole field strength in the equatorial plane at the location of the magnetopause R_{MP} can be estimated as (see eq. (7.15))

$$\begin{aligned} B_{dip} &= B(R_{MP}, 0, 90) \\ &= g_1^0 \left(\frac{R_e}{R_{MP}}\right)^3 \\ &= B_{eq} \left(\frac{R_e}{R_{MP}}\right)^3 \end{aligned} \qquad (7.17)$$

such that we can estimate the stand-off distance of the magnetopause R_{MP} in units of Earth radii (R_e) from solar wind parameters:

$$\frac{R_{MP}}{R_e} = \left(\frac{2B_{eq}^2}{\mu_0 K \rho_{SW} v_{SW}^2}\right)^{1/6}. \qquad (7.18)$$

For typical solar wind conditions we find R_{MP} to be around 10, in good agreement with measurements.